

Monitoring the Corrosion Rate of Copper under a Single Droplet of NaCl

G A. EL-Mahdy^{1,*}, Amro K.F. Dyab^{1,2}, Hamad A. Al-Lohedan¹

¹Chemistry Department, College of Science, King Saud University, P.O.Box - 2455, Riyadh - 11451, Saudi Arabia

² Chemistry Department, Faculty of Science, Minia University 61519, Minia, Egypt.

*E-mail: gamalmah2000@yahoo.com

Received: 27 January 2013 / *Accepted:* 28 February 2013 / *Published:* 1 April 2013

The corrosion rate of copper under a single droplet of NaCl has been investigated using electrochemical impedance spectroscopy technique. The changes in contact angle, volume loss and droplet height during the progress of corrosion process will be monitored. Corrosion rates were greatly accelerated as the droplet height decreases as a result of the decrease of the diffusion layer thickness and did not alter significantly for higher droplet height. The values of the contact angle, droplet height increase as the holding time progresses, while the volume loss increases. The decrease in contact angle with holding time is accompanied by a decrease in the wetting properties of the copper surface with time. A mechanism describing the successive stages of the corrosion process within a droplet is suggested.

Keywords: Copper, EIS, Contact angel, droplet height

1. INTRODUCTION

When a droplet impinges on a metal surface a number of complex and simultaneous interactions are triggered. Interactions of the droplet with a material include chemical and electrochemical interactions, such as dissolution of the native surface oxides, development of pH and O₂ gradients, establishment of electrochemical cells and precipitation of corrosion products [1,2]. The development of new tests and methodologies for the assessment of atmospheric corrosion under thin electrolytic layers is still an important field of research and attracts many researchers to develop the technique. The role of the thickness of the electrolyte layer on the corrosion rate was explained by many researchers [3-15]. It was reported previously that the thickness of the electrolyte layer affected a number of processes, e.g. the accumulation of corrosion products, the mass transport of dissolved

oxygen as well as the hydration of dissolved metal ions [16]. A recent work has been done to explain the local corrosion in an electrolytic droplet rather than in a thin film [17]. Electrochemical Impedance Spectroscopy is a well established technique for the investigation of the atmospheric corrosion of different metals under a thin electrolyte layer [12-3, 18-19]. The concentration and thickness of the thin electrolyte layer on a metal surface exposed to atmospheric conditions change due to the due to the natural processes like water evaporation, and moisture adsorption. Atmospheric corrosion research studies have also used electrolyte droplets to simulate the local environment [17, 20]. The hydrophilicity/ hydrophobicity of a material is usually determined by measuring contact angles of drops of liquid on the material surface. If the material is water-repelling (hydrophobic), a water drop on the surface of a material will have a contact angle, θ , greater than 90 degrees. Otherwise, if the material is water-attracting (hydrophilic), the contact angle will be less than 90 degrees. In our previous work [4, 10, 19] we monitored the changes in corrosion rate under thin electrolyte layers. In this work, the corrosion rate of copper under a single droplet of NaCl will be investigated. The work will extend to monitor the changes in contact angle, volume loss and the height of the droplet during the progress of the corrosion process.

2. EXPERIMENTAL PROCEDURE

2.1. Material and electrode preparation

Two-electrode cell configuration was fabricated from copper sheet (99.99) with dimensions 1mm (width) and 10 mm (length) and embedded parallel in an epoxy resin with 0.1 mm apart from each other. Prior to experiments, the electrode was polished with SiC emery paper down to #2000. The cell containing the two metal plates was set horizontally on an acrylic vessel with the metal surface facing upwards.

2.2 Electrochemical impedance spectroscopy (EIS)

The impedance measurement was conducted at 10 kHz and 10 mHz, using multichannel Solartron system 1470E. The polarization resistance (R_p) was determined by subtracting the high frequency impedance at 10 kHz from the low frequency impedance at 10 mHz.

2.3. Monitoring the droplet characteristics

The changes in contact angle, volume loss and droplet height during the progress of corrosion process will be monitored using a drop shape analysis system (DSA-100, Kruss, Germany) with analysis software DSA4 software (V.1.0-03).

2.3. Corrosion products Morphology

The morphology of the corrosion products was examined by utilizing optical microscopy (Olympus BX-53) fitted with DP72 digital camera). Images were processed using Olympus CellSens v1.6.

3. RESULTS AND DISCUSSION

3.1. Monitoring the corrosion rate

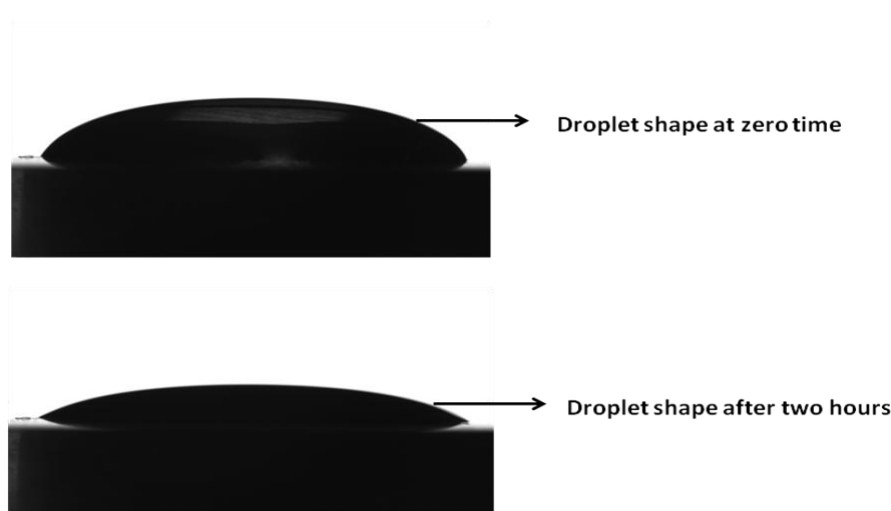


Figure 1. Droplet shape at zero time and after 2 hours.

A single droplet of 0.5M NaCl was placed horizontally as shown in Fig. 1. The polarization resistance (R_p) between two frequency points (10 mHz and 10KHz) was monitored using EIS technique. The corrosion rate is proportional to the reciprocal of polarization resistance and can be calculated using the Stern–Geary equation [21]:

$$\text{Corrosion rate} = K / R_p \quad (1)$$

$$K = \frac{b_a b_c}{2.303(b_a + b_c)} \quad (2)$$

where b_a and b_c represent anodic and cathodic Tafel slope, respectively. The value of K is a function of metal and electrolyte [4,10,19] and can be assumed to be constant for a given metal/electrolyte system. Previously, EIS technique was successively applied to monitor the corrosion rate of the steel, coated steel and metals under wet–dry cyclic condition and thin electrolyte layer [12–13, 22–24]. The monitoring data is shown in Fig. 2. The corrosion process can be divided into two distinct regions. The first region is characterized by dissolution of oxide film followed by metal dissolution. The corrosion process is controlled by anodic dissolution in this region and the behavior is

similar to the behavior of the metal in bulk solution. In region II, the corrosion rate sharply increases as time progresses.

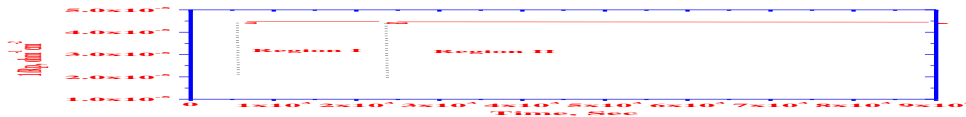


Figure 2. Variation of reciprocal of polarization resistance ($1/R_p$) with time.

The results can be explained on the basis of thinning process of the droplet due to evaporation process, which accompanied by an increase in NaCl concentration and decreasing the droplet height. As the droplet height decreases the corrosion process occurred under thin electrolyte layers and is controlled by oxygen reduction, which enhanced by diffusion of oxygen through a shorter path when the droplet height decreases.

3.2. Monitoring the Contact angles

Contact angles contain information about hydrophilicity or hydrophobicity of a surface, which plays an important role in the interaction of the liquid with exposed surface. Fig.3 shows the monitoring data of contact angle with holding time. It is clear that contact angle decreases with time from 85° to 24° due to the evaporation of the water as time progressed. The observed fluctuations in contact angle values during the last stage of monitoring can be attributed to the roughness of the surface due to the precipitation and dissolution of the corrosion products. In addition, deposition of NaCl crystals may form an insulating layer, which acts as a new substrate and give rise to more error in contact angle measurements. During the last stage of droplet drying, the contact angle is not related to the wettability, especially after complete drying. It can be concluded that the decrease in contact angle with holding time is accompanied by decreasing the surface energy and the wetting properties of the copper surface with time.

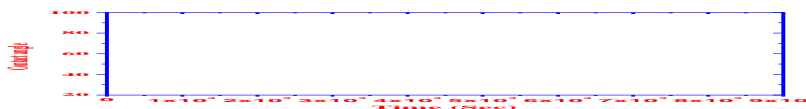


Figure 3. Dependence of contact angle on holding time.

3.3. Monitoring the volume loss and the droplet height

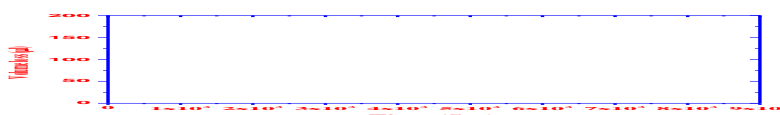


Figure 4. Changes of volume loss with holding time.

Monitoring data of volume loss and droplet height with holding time are shown in Figures 4 and 5, respectively. The volume loss increases linearly with time, while the droplet height decreases.

During evaporation, the droplet height decreased and its concentration increased. The increase in volume loss could be attributed to an increase in the amount of water evaporation in the droplet or the consumption of the droplet by the corrosion reaction and is accompanied by a decrease in droplet height.

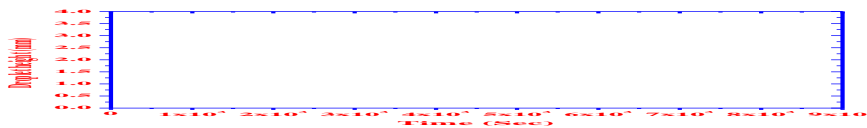
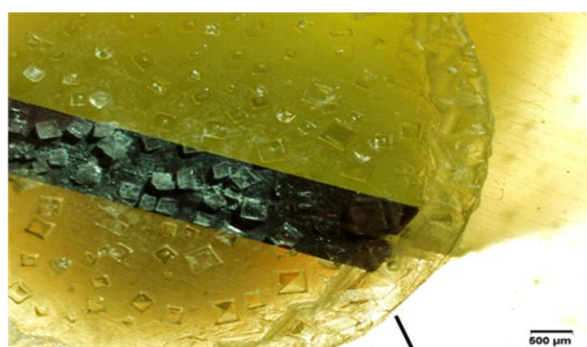


Figure 5. Variation of droplet height ($1/R_p$) with time.



circular contact
area formed from NaCl
crystals

Figure 6. Photomicrograph representing the circular contact area after complete drying of the droplet.

This might indicate the corrosion progression between the droplet and the copper surface increases. The height of the electrolyte drop decreases with holding time (Fig. 5) due to the loss in droplet volume as a result of water evaporation or the consumption of the droplet by the corrosion reaction. The droplet height can influence the rate of oxygen reduction when the rate is under diffusion control and has no effect for higher droplet height because the rate of corrosion is under anodic control. It can be concluded that the droplet height decreased as time progressed, while the circular contact area of the droplet did not change during drying as evident from photomicrograph shown in Fig 6. The results are in good agreement with that reported previously by Maier and Frankel [25] and Hastuty et al. [26].

3.4. Corrosion products morphology

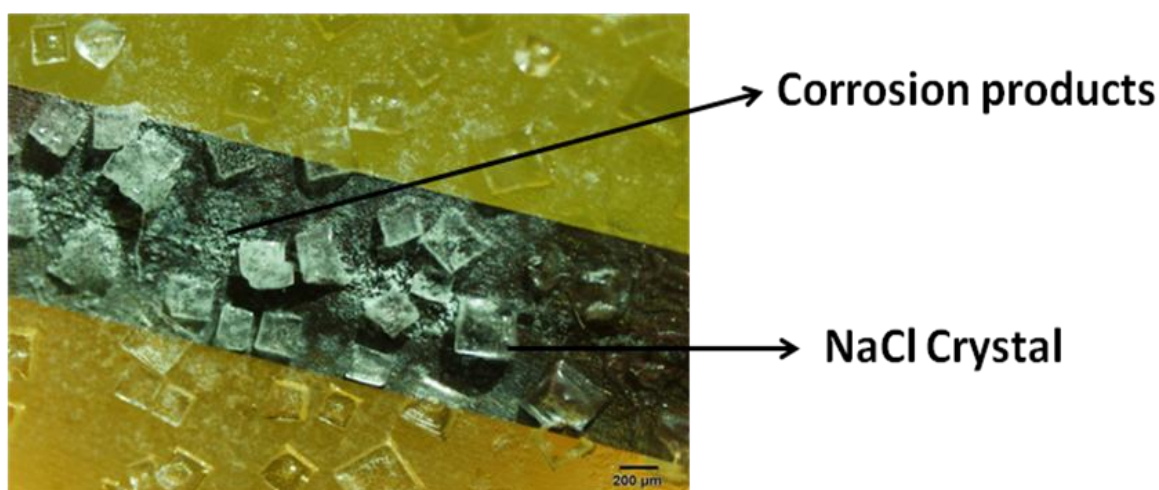


Figure 7. Photomicrograph representing the distributions of the corrosion products on the copper surface after complete drying of the droplet.

The morphology of the corrosion products after 4 hours is shown in Fig. 7. It is clear that heavy corrosion products are observed in the centre and secondary spread regions. Droplets have been dried to be a solid corrosion product by a corrosion reaction between the copper, or the corrosion reaction has almost been finished and the droplet has turned out to be a solid corrosion product with almost the same shape as the original droplet. It is expected that the center remains acidic, while the peripheral region will be slightly alkaline due to the reduction of O_2 . It can be seen also the formation of NaCl crystals after complete droplet evaporation. Corrosion products and salts form in the central, peripheral and secondary spread regions as the droplet evaporates. Various crystalline phases of corrosion products have been identified previously for copper corrosion in NaCl solution using XRD [23]. The main oxide identified in the corrosion products is Cu_2O [23]. It can be seen that the major corrosion products distributed over the central, peripheral and secondary spread regions are Cu_2O , $Cu_2(OH)_3Cl$ and Cu_2Cl [23].

3.5. Corrosion Mechanism within a droplet

As corrosion commences, electrochemical reactions become spatially separated due to differential diffusion of O₂. The anodic reactions established near the centre of a droplet, while and the cathodic reactions occurring at the edge of the droplet [1, 27-28]. The anodic dissolution of copper occurs within a droplet of higher height as in region I (Fig. 2) as follows:



Due to variant and evolving local conditions within a droplet, a distinct oxide (Cu₂O) may develop in spatially different location. As the time progresses the height of droplet decreases and the concentration of the NaCl increases, which is accompanied by an increase in corrosion rate as observed in region II (Fig. 2). The corrosion process in this region can be described by a reduction of oxygen as:



The peripheral region will develop an alkaline pH due to the reduction of O₂ to hydroxyl ions [7]. The development of pH and ion concentration gradients can lead to the formation of other products as Cu₂(OH)₃Cl and Cu₂Cl [23]. During the last stage of evaporation the concentration of dissolved salt progressively increase towards saturation, with the precipitation of corrosion products as Cu₂O, Cu₂(OH)₃Cl and Cu₂Cl as shown in Fig. 7, which shows the images of the corrosion products after complete drying.

4. CONCLUSIONS

- 1- The electrochemical impedance spectroscopy is a powerful technique for determination the corrosion rate under a single droplet.
- 2- The experimental set up has been proven to be a useful for gaining detailed about droplet electrochemistry.
- 3- Corrosion rates were greatly accelerated as the droplet height decreases and did not alter significantly for higher height droplet.
- 4- The droplet height decreases as time progresses, while the circular contact area of the droplet did not change after complete drying

ACKNOWLEDGMENT

The project was supported by the Research Center, College of Science, King Saud University.

References

1. A.K. Neufeld, I.S. Cole, A.M. Bond, S.A. Furman, *Corros. Sci.* 44 (2002) 555.
2. T.E. Graedel, *J. Electrochem. Soc.* 136 (1989) 193C.

3. N.D. Tomashov, *Corrosion* 20 (1964) 7.
4. G.A. El-Mahdy, *Corrosion* 59 (2003) 505.
5. M. Stratmann, H. Streckel, *Corros. Sci.* 30 (1990) 681.
6. M. Stratmann, H. Streckel, K.T. Kim, S. Crockett, *Corros. Sci.*(1990) 715.
7. T. Tsuru, K.-I. Tamiya, A. Nishikata, *Electrochim. Acta* 49 (2004)2709.
8. A.K. Neufeld, L.S. Cole, A.M. Bond, S.A. Furman, *Corros. Sci.* 44(2002) 555.
9. R.P. Cruz Vera, A. Nishikata, T. Tsuru, *Corros. Sci.* 38 (1996)1397.
10. G.A. El-Mahdy, A. Nishikata, T. Tsuru, *Corros. Sci.* 42 (2000)183.
11. A. Nazarov, D. Thierry, *Electrochim. Acta* 49 (2004) 2717.
12. A. Nishikata, S. Kurnagai, T. Tsu, *Corr. Eng.* 43 (1994) 109.
13. A. Nishikata, T. Takahashi, B. Horu, T. Tsuru, *Corros. Eng.* 43(1994) 225.
14. Q. Qu, C.i. Yan, Y. Wan, C. Cao, *Corros. Sci.* 44 (2002) 2789.
15. A.P. Yadav, A. Nishikata, T. Tsuru, *Corros. Sci.* 46 (2004) 361.
16. A. Nishikata, Y. Ichihara, Y. Hayashi, T. Tsuru, *J. Electrochem. Soc.*144 (1997) 1244.
17. E. Dubuisson, Philippe Lavie, Francis Dalard, Jean-Pierre Caire, Sabine Szunerits, *Corros. Sci.* 49 (2007) 910–919..
18. R.P. Vera Cruz, A. Nishikata, T. Tsuru, *Corros. Sci.* 38 (1996) 1397.
19. G.A. El-Mahdy, A. Nishikata, T. Tsuru, *Corros. Sci.* 42 (2000) 1509.
20. E. Dubuisson, P. Lavie, F. Dalard, J.P. Caire, S. Szunerits, *Electrochem. Commun.* 8 (2006) 911–915.
21. M. Stern, A.L. Geary, *J. Electrochem.* 104 (1957) 56.
22. A. Nishikata, Y. Yamashita, H. Katayama, T. Tsuru, A. Usami, T.Tanabe, *Corros. Sci.* 37 (1995) 2059.
23. G.A. EL-Mahdy , *Corros. Sci.* 47 (2005) 1370–1383
24. G.A. EL-Mahdy and K. B. Kim *Electrochim. Acta* 49 (2004) 1937.
25. B. Maier, G.S. Frankel, *J. Electrochem. Soc.* 157 (2010) C302–C312.
26. S. Hastuty, A. Nishikata, T. Tsuru, *Corros. Sci.* 52 (2010) 2035.
27. I.S. Cole, N.S. Azmat, A. Kanta, M. Venkatraman, *Int. Mater. Rev.* 54 (2009) 117.
28. N.S. Azmat, K.D. Ralston, I.S. Cole, *Surf. Coat. Tech.* 205 (2010) 928.